

Ultrastructural characterization of host–parasite interactions of *Plasmodium coatneyi* in rhesus macaques

Research Article

Cite this article: Lombardini ED, Malleret B, Rungojn A, Popruk N, Kaewamatawong T, Brown AE, Turner GDH, Russell B, Ferguson DJP (2022). Ultrastructural characterization of host–parasite interactions of *Plasmodium coatneyi* in rhesus macaques. *Parasitology* **149**, 161–170. <https://doi.org/10.1017/S0031182021001669>

Received: 3 May 2021

Revised: 15 July 2021

Accepted: 20 September 2021

First published online: 4 October 2021



Key words:

Malaria; *Plasmodium coatneyi*; *Plasmodium falciparum*; rhesus macaque; sequestration; ultrastructure

Author for correspondence:

E. D. Lombardini,

E-mail: Eric.lombardini.mil@afirms.org

E. D. Lombardini¹ , B. Malleret^{2,3} , A. Rungojn^{4,5}, N. Popruk¹, T. Kaewamatawong⁶, A. E. Brown⁷, G. D. H. Turner^{4,5}, B. Russell⁸ and D. J. P. Ferguson^{9,10}

¹Department of Veterinary Medicine, Armed Forces Research Institute of Medical Sciences (AFRIMS), Bangkok, Thailand; ²Department of Microbiology and Immunology, Immunology Translational Research Programme, Yong Loo Lin School of Medicine, Immunology Programme, Life Sciences Institute, National University of Singapore, 117597 Singapore, Singapore; ³Singapore Immunology Network (SigN), Agency for Science & Technology, Singapore, Singapore; ⁴Mahidol Oxford Clinical Research Unit, Faculty of Tropical Medicine, Mahidol University, Bangkok, Thailand; ⁵Nuffield Department of Medicine, Centre for Tropical Medicine, University of Oxford, Oxford, UK; ⁶Department of Veterinary Pathology, Chulalongkorn University, Bangkok, Thailand; ⁷Faculty of Medical Technology, Mahidol University, Salaya, Thailand; ⁸Department of Microbiology and Immunology, University of Otago, Dunedin, New Zealand; ⁹Nuffield Department of Clinical Laboratory Sciences, University of Oxford, John Radcliffe Hospital, Oxford, UK and ¹⁰Department Biological & Medical Sciences, Oxford Brookes University, Oxford, UK

Abstract

Plasmodium coatneyi has been proposed as an animal model for human *Plasmodium falciparum* malaria as it appears to replicate many aspects of pathogenesis and clinical symptomology. As part of the ongoing evaluation of the rhesus macaque model of severe malaria, a detailed ultrastructural analysis of the interaction between the parasite and both the host erythrocytes and the microvasculature was undertaken. Tissue (brain, heart and kidney) from splenectomized rhesus macaques and blood from spleen-intact animals infected with *P. coatneyi* were examined by electron microscopy. In all three tissues, similar interactions (sequestration) between infected red blood cells (iRBC) and blood vessels were observed with evidence of rosette and auto-agglutinate formation. The iRBCs possessed caveolae similar to *P. vivax* and knob-like structures similar to *P. falciparum*. However, the knobs often appeared incompletely formed in the splenectomized animals in contrast to the intact knobs exhibited by spleen intact animals. *Plasmodium coatneyi* infection in the monkey replicates many of the ultrastructural features particularly associated with *P. falciparum* in humans and as such supports its use as a suitable animal model. However, the possible effect on host–parasite interactions and the pathogenesis of disease due to the use of splenectomized animals needs to be taken into consideration.

Introduction

Plasmodium coatneyi is an agent of malaria that infects a variety of old-world monkeys in South East Asia. The parasite was first identified in 1961 in an Anopheles mosquito from Malaya (Eyles *et al.*, 1962). Subsequently, its complete lifecycle was described following experimental inoculation into a rhesus macaque. The species has been reported as part of a survey of blood parasites in cynomolgus macaques (*Macaca fascicularis*) which was conducted in the Philippines and resulted in significant interest in the use of the parasite as a model for severe human malaria associated with *Plasmodium falciparum* (Eyles *et al.*, 1962, 1963; Aikawa *et al.*, 1992; Kawai *et al.*, 1993; Moreno *et al.*, 2013; Lombardini *et al.*, 2015).

The plasmodial parasites of Cercopithecidae monkeys from Asia are comprised of 10 species including *P. coatneyi* and the closely related *Plasmodium knowlsei*. This group also includes *Plasmodium gonderi*, infectious to Cercopithecidae from Africa; *Plasmodium hylobati*, which parasitizes Hylobatidae monkeys from Asia; and *Plasmodium vivax* (Escalante *et al.*, 1995; Leclerc *et al.*, 2004; Hayakawa *et al.*, 2008; Lombardini *et al.*, 2015).

While not closely related to *P. falciparum*, *P. coatneyi* has a range of biological features that it shares with *P. falciparum* as well as several important distinguishing phenotypic traits: Both parasites have an erythrocytic stage with a 48-hour cycle (Eyles *et al.*, 1971), there is evidence of microvascular cytoadherence, with the formation of rosettes between infected erythrocytes and uninfected red blood cells and several early reports have described the development of electron-dense knobs on the cell surface of infected erythrocytes which have been purported to be involved in cytoadhesion (Kilejian *et al.*, 1977; Aikawa *et al.*, 1992; Lombardini *et al.*, 2015). Furthermore, both *P. falciparum* and *P. coatneyi* undergo deep vascular sequestration of red blood cells infected with trophozoites and schizonts (Desowitz *et al.*, 1969; MacPherson *et al.*, 1985; Pongponratn *et al.*, 1991; Sein *et al.*, 1993; Smith *et al.*, 1996).

Plasmodium coatneyi has been reported as causing both natural and experimentally induced disease in a variety of non-human primate species (Kawai *et al.*, 1993, 1998; Sein

et al., 1993; Smith *et al.*, 1996; Moreno *et al.*, 2013; Lombardini *et al.*, 2015). The cynomolgus macaque is described as being one of the natural hosts of the parasite and it is theorized that the parasite may have coevolved with the cynomolgus, resulting in reduced clinical disease in comparison with experimental infections in the rhesus or the Japanese macaque (Eyles *et al.*, 1971; Kawai *et al.*, 1993, 1995, 1998; Moreno *et al.*, 2013; Lombardini *et al.*, 2015). Tissue pathology associated with *P. coatneyi* infection in the rhesus macaque is variable and likely is dependent on the genetic heterogeneity of the infected population, degree of blood parasitaemia, coinfection with other agents, immune status, age and overall health of the animals (Lombardini *et al.*, 2015, 2021).

A large project has been undertaken in order to evaluate many aspects of the pathology of *P. coatneyi* in rhesus macaques and to evaluate its potential as a model for human falciparum malaria. In the present study, the ultrastructural features of *P. coatneyi* infected red blood cells (iRBC) and their in-situ interaction with host tissue are described. The features identified will be directly compared to those of *P. falciparum* infections in humans as were previously examined using identical techniques (Pongponratn *et al.*, 2003).

Materials and methods

Six splenectomized Indian origin rhesus macaque monkeys were used in two studies in 2013 and 2014 at the Armed Forces Research Institute of Medical Sciences (AFRIMS) (Lombardini *et al.*, 2015, 2021), in addition to the inclusion of two spleen intact animals in 2015. The research was conducted in compliance with the Animal Welfare Act and other federal statutes and regulations relating to animals and experiments involving animals and adhered to principles stated in the *Guide for the Care and Use of Laboratory Animals*, NRC Publication, 2011 edition. All animal use was approved by the AFRIMS Institutional Animal Care and Use Committee Protocol Number 12-08. The splenectomized experimental animals were comprised of four adult males and two adult females, while the spleen intact animals were both females. The mean age of the male animals was 11.7 years, and the mean weight was 11 pounds. The mean age of the female animals was 10 years and the mean weight was 12 pounds. The first six animals were enrolled in pathophysiology and model refinement study in which parasitaemia levels and parasite staging were conducted every other hour for the 3 days associated with peak parasitaemia (Lombardini *et al.*, 2015). In all instances, the experimental animals were inoculated from one donor rhesus to another through a blood challenge of *P. coatneyi* infected erythrocytes. Inoculation began in an infected donor by intravenous inoculation of freshly thawed cryopreserved *P. coatneyi* strain infected blood. The stabilate stock used was the Hackeri strain of *P. coatneyi* archived at AFRIMS, thereby ensuring that the stain of plasmodium was homogenous and standardized across the experimental animals. Once the parasitaemia in donor animals had reached >50 000 parasitized RBCs per μL , 10–20 mL of blood was drawn into a heparinized tube, diluted with sterile PBS solution to a concentration of 5×10^6 infected erythrocytes per 1 mL suspension, and divided into equal 1 mL aliquots. These 1 mL aliquots were subsequently used to infect the study animals *via* intravenous inoculation. In accordance with the approved protocol, animals were euthanized based on the combined criteria of parasitaemia levels of 20% or greater, blood values and clinical signs. In these animals, comprehensive autopsies were performed with the collection of all tissues immediately post-mortem. All tissues were processed for histopathological, immunohistochemical and ultrastructural analyses using a standardized tissue sampling protocol (Lombardini *et al.*, 2015). Tissues sampled included multiple areas of the central nervous

system (thalamus, hippocampus, forebrain, cerebellum, brain stem, spinal cord), kidneys and heart in all six experimental animals. At autopsy, tissue samples were collected from target organs, trimmed into $\sim 1 \text{ mm}^3$ blocks which were immersed within 1 min of collection in 2.5% glutaraldehyde in 0.1 M phosphate buffer and subsequently processed for routine transmission electron microscopy (TEM). In summary, samples were post-fixed in osmium tetroxide, dehydrated and embedded in Spurr's epoxy resin (TABB Limited UK). Thin sections of areas of interest were cut to a thickness of approximately 70 nm, and stained with uranyl acetate and lead citrate, and subsequently, grids were examined in a JEOL 1200EX electron microscope (JEOL UK). This process was similar to that described previously for a human autopsy study of fatal *P. falciparum* malaria (Pongponratn *et al.*, 2003).

In addition, the blood from two spleen intact animals infected with *P. coatneyi* was obtained once parasitaemia was achieved and processed for both transmission and scanning electron microscopy. These animals underwent curative treatment. For TEM, the cells were centrifuged and the pellet fixed in 2.5% glutaraldehyde in 0.1 M phosphate buffer and processed for routine TEM as described above. Scanning electron microscopy (SEM) was conducted on *P. coatneyi* infected red cells after magnetic enrichment, using standard SEM protocols as in Malleret *et al.* (2013). Briefly, sorted cells were allowed to settle on a poly-lysine (Sigma) pre-treated glass coverslip for 15 min at room temperature (RT) prior to fixing in glutaraldehyde and post-fixing in osmium tetroxide (as described above). After washing in deionized water, cells were dehydrated and critical point dried. Samples were sputter-coated with gold prior to examination with a field emission scanning electron microscope (JSM-6701F, JEOL).

Microscopic enumeration of iRBCs was performed using thin blood smears stained with Giemsa. A minimum of 4000 RBCs were counted (20 fields at 100 \times magnification). Live cell subvital staining of reticulocytes and of parasites was done using Giemsa (Lee *et al.*, 2013).

Results

Tissue samples

Ultrastructural examination of grids from the three selected tissues (brain, kidney and heart) from the six experimental animals, allowed for evaluation of the distribution of iRBC within the deep microvasculature. Counting the percentage of iRBCs to uninfected RBCs in each tissue gave 41% in the brain, 46% in the heart muscle and 38% in the kidney (based on a minimum of 12 blood vessels and over 120 erythrocytes for each tissue). There was a very strong synchrony of parasite stage of maturation and as such, the vast majority of the observed parasites were trophozoites characterized by their spherical appearance with cytoplasm containing a nucleus and food vacuole (Figs 1, 2A, B, 3B and C). Only a relatively few mature schizonts (Fig. 3A) and ring forms were observed. In all three tissues, iRBCs were identified in both large and small blood vessels with no obvious difference in the number or appearances of iRBCs between tissues (Figs 1–3).

The smaller blood vessels were typically tightly packed with a mixture of uninfected and infected erythrocytes (Figs 1–3). While the majority of infected cells had a single parasite, a number had multiple parasites (Figs 1A and 3C). The parasites were located within a parasitophorous vacuole limited by a unit membrane (Fig. 2G). Trophozoites appeared to increase in size, developing from stages with a single nucleus (Fig. 2A) to stages with multiple nuclei and finally into mature schizonts (Fig. 3A). Food vacuoles were initially small but increased in size into large vacuoles containing a number of hemozoin crystals (Figs 2B and 3A). The few

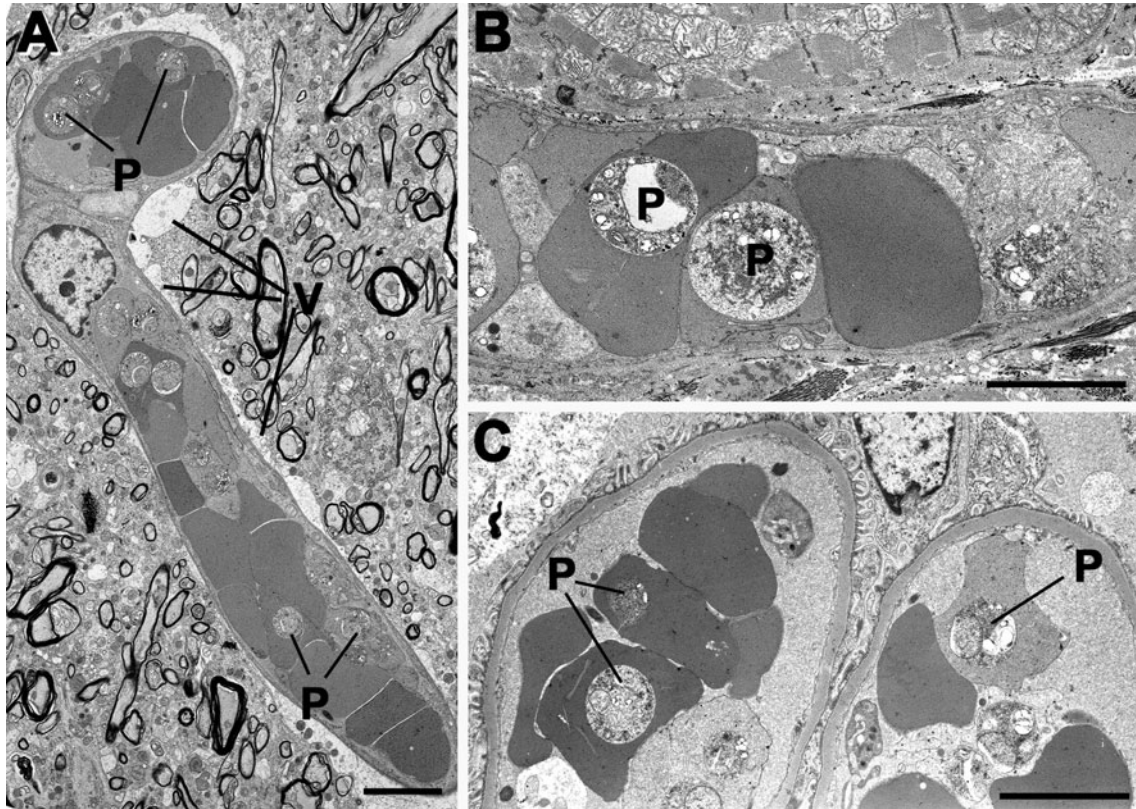


Fig. 1. (A–C) Low power transmission electron micrographs of tissue from *Plasmodium coatneyi* infected splenectomized animals showing the distribution of iRBCs within the blood vessels of the brain (A) heart (B) and the glomerulus of a kidney (C). Note the cytoplasmic vacuolation (V) around the cerebral blood vessel. P – *Plasmodium coatneyi* parasite. Bars are 10 μ m.

mature schizonts were comprised of multiple merozoites, with apical rhoptries and a posterior nucleus, centred around a body of residual cytoplasm containing food vacuoles filled with hemozoin crystals (Fig. 3A). The erythrocytic cytoplasm frequently contained numbers of circular or curved bilayered channels interpreted as tubular vesicular structures with a narrow electron-lucent lumen (Fig. 2B insert). However, Maurer's clefts running parallel to the RBC plasmalemma, characteristic for *P. falciparum* iRBCs, were not observed. The majority of iRBCs within small blood vessels were more spherical in shape with a relatively regular outline (Figs 1A and 2B). However, others show marked deformation of shape consisting of irregular cytoplasmic protrusions giving the infected cells a more flattened, crenated appearance (Figs 2A and 3B). A feature of all iRBCs was the presence of a number of caveolae, which measured approximately 90 nm in diameter described as small spherical invaginations with an electron-dense internal coating but with no evidence of associated vesicles (Figs 2A–C). In addition, a variable number of blebs or excrescences consistent with knob formation were observed. These knob-like structures were 70–90 nm in diameter (Fig. 2C, E and H). However, detailed examination showed that while a few possessed some electron-dense material beneath the plasmalemma (Fig. 2C), the majority (>60%) appeared to lack the clearly defined sub-plasma membrane electron-dense material (Fig. 2G). In addition, it was also possible to identify rare (<10%) plaques of electron-dense material associated with the iRBC plasmalemma but lacking protuberance (Fig. 2D). The majority of iRBCs appeared to have relatively few knobs irrespective of the stage of parasite development, and those that were noted appeared to be randomly distributed. In addition, examination of numerous (50+) iRBCs did not appear to demonstrate knob number as being related to the stage of parasite development.

In small vessels, there was often a tight association between the iRBC and endothelial cells (Fig. 2B and G), which resulted in evidence of margination of iRBCs along the luminal wall (Fig. 2A). When examined in detail there appeared to be close apposition between the iRBC plasmalemma and the plasmalemma of the endothelial cells with areas showing possible connection *via* proteinaceous material (Fig. 2B and G). While in the majority of cases, knob-like protuberances were absent from such areas, they were observed on occasion. In these cases, proteinaceous-like material connecting the knob to the endothelial surface was observed (Fig. 2H). Also, there was evidence of limited microvillus formation by the endothelial cells with a cytoplasmic process protruding into invaginations of the iRBC surface (Fig. 2F). In the larger vessels, where the RBCs were more loosely packed, it was often possible to observe clumping of iRBCs consistent with possible auto-agglutination (Fig. 3B) and interactions between iRBCs and RBCs possibly related to rosette formation (Fig. 3C). The iRBCs in this situation showed more severe shape changes and there was less evidence of cytoadherence between iRBCs and the endothelium in such vessels. No example of vessel rupture was observed by electron microscopy, although several endothelial cells showed some degenerative changes. There did appear to be lucent and vacuolated areas around certain cerebral vessels, which were interpreted as oedema (Fig. 1A). Within the vessels, a number of macrophages and neutrophils were observed and certain macrophages appear to have phagocytosed packets of malarial pigment (Fig. 3D).

Blood samples

The observation of anomalies on the structure of the knob described above in splenectomized animals was unexpected. Therefore, to see if this was a phenomenon arising from the

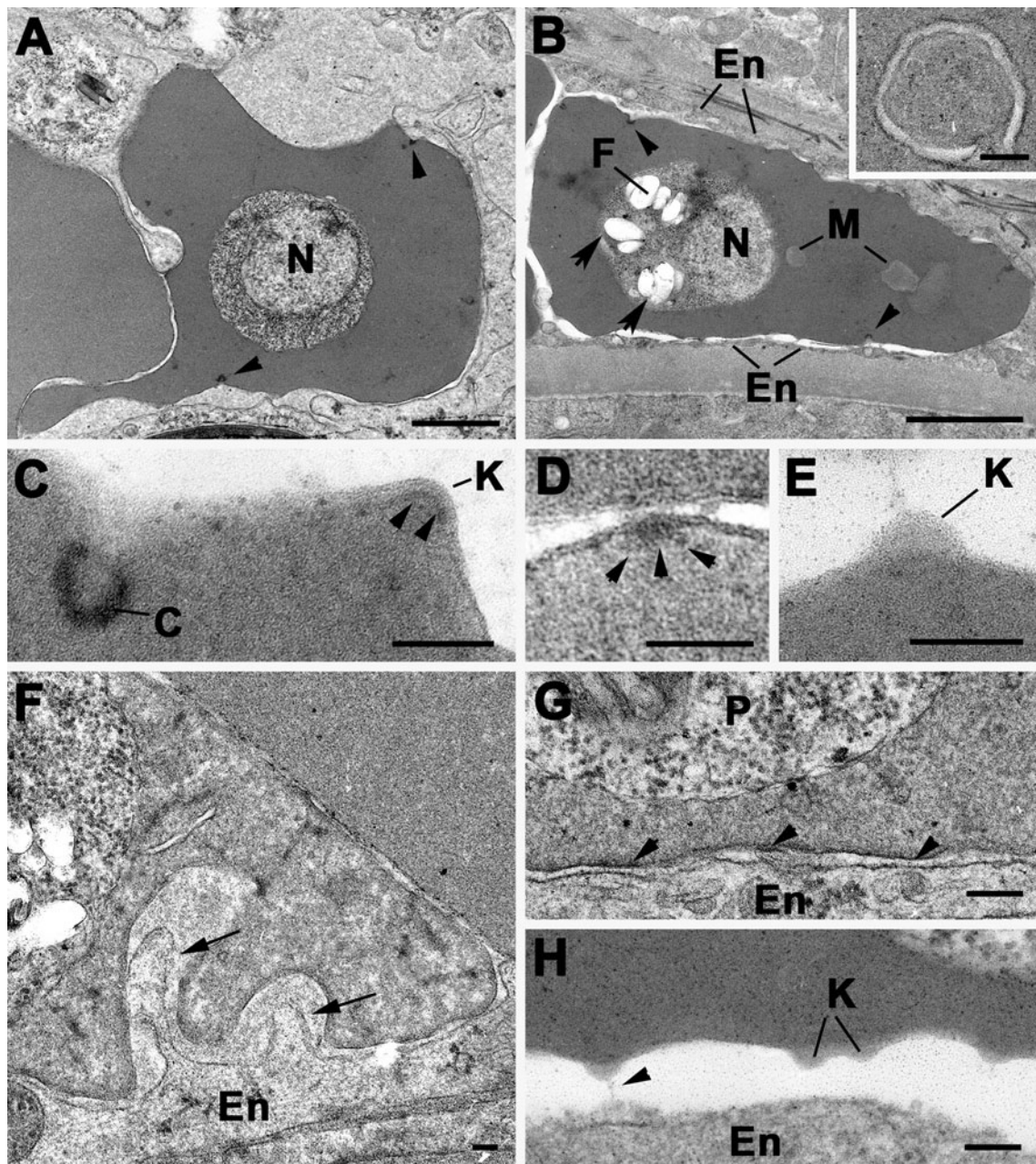


Fig. 2. Transmission electron micrographs showing the structure of *Plasmodium coatneyi* iRBCs and their relationship to host endothelial cells. (A) Section through an iRBC showing a trophozoite with a centrally located nucleus (N). Note that the surface of the iRBC exhibits caveola formation (arrowheads). Bar is 1 μm . (B) iRBC with a trophozoite displaying a nucleus (N) and hemazoin crystals (arrows) in the food vacuole (F). There are also membrane structures (M) in the cytoplasm and caveola (arrowheads) at the plasmalemma of the iRBC. Note the tight apposition of the iRBC plasmalemma with the endothelial cells (En) lining the vessel. Bar is 1 μm . Inset: Detail of part of the cytoplasm of a similarly infected RBC's cytoplasm showing the double membrane-bound tubular structure. Bar is 100 nm. (C) Detail from the surface of an iRBC showing an invagination of the plasmalemma to form a caveola (C) with underlying electron-dense material and a knob (K) with underlying dense material (arrowheads). Bar is 100 nm. (D) Detail from the surface of an iRBC in which electron-dense material (arrowheads) is associated with the plasmalemma of an iRBC but in the absence of any protrusion. Bar is 100 nm. (E) Detail from the surface of an iRBC showing a knob (K) that appears to lack underlying dense material. Bar is 100 nm. (F) Section through the junction between an iRBC and an endothelial cell (En) showing two microvilli from the endothelial cell protruding into folds in the iRBC (arrows). Bar is 1 μm . (G) Enlargement of the junction between iRBC and endothelial cell (En) with no evidence of knob formation but proteinaceous-like material appearing to connect the plasma membranes (arrowheads). P – parasite. Bar is 100 nm. (H) Detail of junction between iRBC and endothelial cell (En) where the iRBC appears to form knobs (K). Note the proteinaceous-like material (arrowhead) connecting the knob to the endothelial cell (En). Bar is 100 nm.

specific use of splenectomized animals, blood was obtained from femoral arteries in two spleen-intact animals infected with *P. coatneyi* and was examined by both TEM and SEM. In these blood samples, it was observed that the iRBCs could be identified by a markedly irregular outline (Fig. 4A and B). By SEM and TEM, the surface of the iRBCs showed the formation of variable numbers of caveolae and knob-like structures (Fig. 4A–F). The structure of the caveolae with the invagination of the plasmalemma with underlying electron-dense material could be seen by TEM

(Fig. 4F) and appeared as surface pores by SEM (Fig. 4B). Detailed examination of the knob-like structures revealed circular electron-dense plaques beneath the plasmalemma shown in the longitudinal section (Fig. 4D) and tangential section (Fig. 2E). The knobs could be identified in SEM as slightly circular electron-lucent structures, which appeared to be random distribution (Fig. 4A and B). Spontaneous rosette formation with normocytes and reticulocytes were observed in wet Giemsa preparations (Fig. 5A) and by SEM (Fig. 5B).

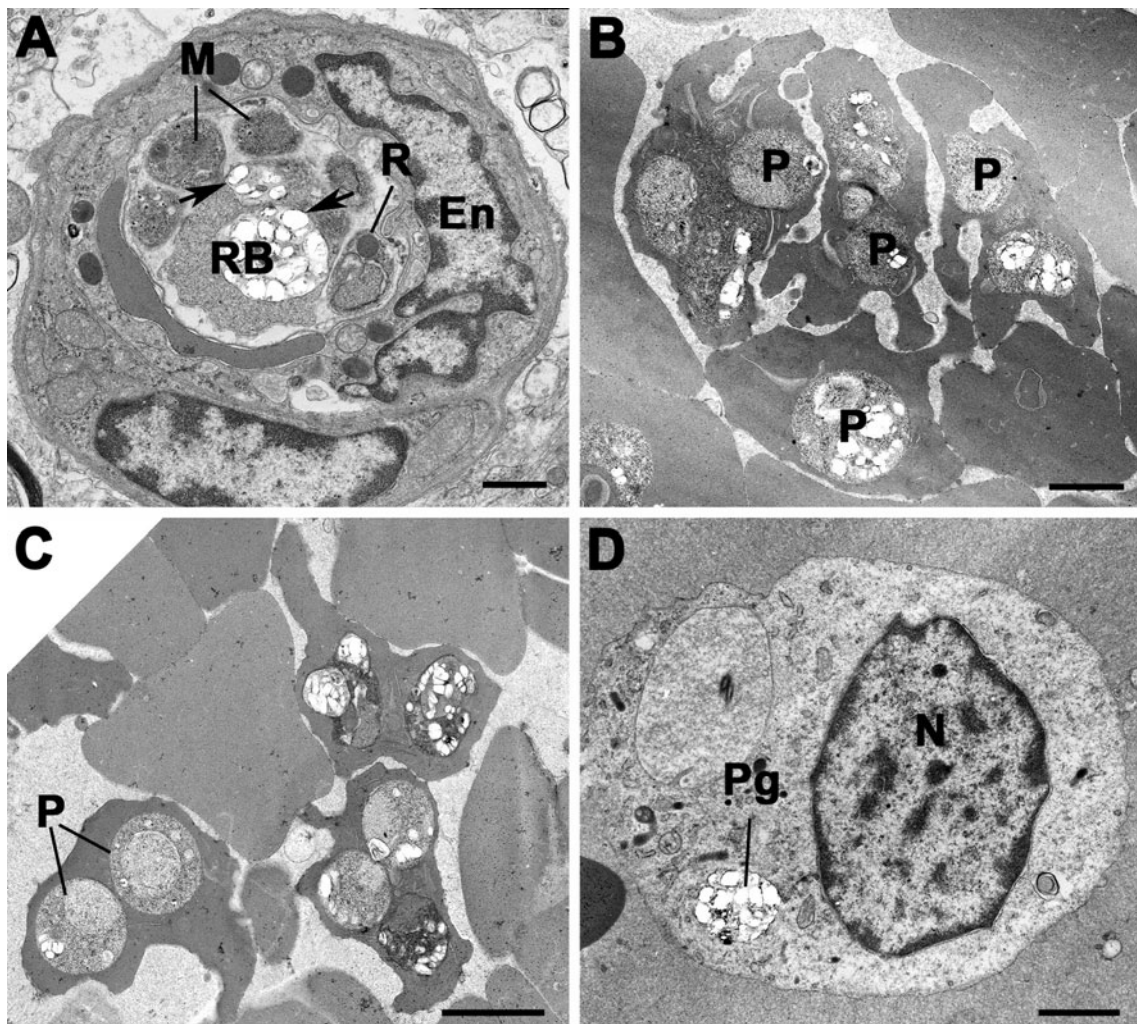


Fig. 3. Transmission electron micrographs of *Plasmodium coatneyi* infected rhesus macaque tissues. (A) Cross-section through a small blood vessel showing an iRBC containing a mature schizont. Note the merozoites (M) with electron-dense rophtries (R) around a residual cytoplasmic mass (RB), as well as hemazoin crystals (arrows). En – endothelial cell. Bar is 1 μ m. (B) Low power from a large vessel showing a number of iRBCs interacting to form an auto-agglutinate-like structure. P – parasite. Bar is 1 μ m. (C) Part of a vessel in which iRBCs are interacting with RBCs to form rosette-like structures. P – parasites. Bar is 1 μ m. (D) Section through a vessel showing macrophage that had phagocytose a packet of pigment (Pg). N-Nucleus. Bar is 1 μ m.

Discussion

To date the majority of studies on *P. coatneyi* have concentrated on the use of the rhesus macaque model as a platform for cerebral malaria studies but with limited morphological evaluation (Kilejian *et al.*, 1977; Aikawa *et al.*, 1992; Kawai *et al.*, 1993; Maeno *et al.*, 1993; Tegoshi *et al.*, 1993; Moreno *et al.*, 2013; Lombardini *et al.*, 2015). The present ultrastructural study was based on the examination of three tissues (brain, heart and kidney) in *P. coatneyi* infected splenectomized animals. Interestingly, quantitative comparisons of the level of sequestration in these three tissues, noted no tissue-specific differences. Prior studies have demonstrated that there is a significant amount of sequestration in the brain of macaques infected with *P. coatneyi* (Desowitz *et al.*, 1969; Sein *et al.*, 1993; Smith *et al.*, 1996; Lombardini *et al.*, 2021). However, the more diffuse tissue sequestration observed in the rhesus model differs from *P. falciparum* in humans where the disease is associated specifically with brain sequestration (MacPherson *et al.*, 1985; Pongponratn *et al.*, 1991, 2003; Nguansangiam *et al.*, 2007).

The changes to the host RBC associated with infection are the formation of tubular/vacuolar structures within cytoplasm and caveolae and knob-like protuberances at the red cell surface. The tubular/vesicular structures appear to be common to all species while caveolae and knobs appear species-specific and

P. coatneyi is unusual in displaying both features. The caveolae observed for *P. coatneyi* are simple invaginations and lack the complex budding and associated vesicles that are characteristic of the caveola-vesicle complexes (CVC) associated with *P. vivax* and *P. knowlseyi* iRBCs (Aikawa *et al.*, 1975; Aikawa, 1988a, 1988b; Barnwell *et al.*, 1990; Akinyi *et al.*, 2012; Liu *et al.*, 2019). Interestingly, both species are phylogenetically more closely related to *P. coatneyi* than is *P. falciparum* (LeClerc *et al.*, 2004; Hayakawa *et al.*, 2008). However, the role of these structures is still unclear although a number of proteins have been localized to the CVC (Udagama *et al.*, 1988). As such their role in *P. coatneyi* is also uncertain. The presence of knobs and the cytoadherence of iRBCs to endothelial cells is similar that seen in *P. falciparum* iRBCs (Aikawa *et al.*, 1983, 1985; Aikawa, 1988a, 1988b; Atkinson and Aikawa, 1990; Bannister *et al.*, 2000; Pongponratn *et al.*, 2003). However, the iRBCs in *P. coatneyi* differ from *P. falciparum* due to the absence of Maurer's clefts beneath the RBC plasmalemma (Bannister *et al.*, 2000; Mundwiler-Pachlatko and Beck, 2013). The presence of the characteristic features of both *P. falciparum* (knobs) and *P. vivax* (caveolae) iRBCs makes *P. coatneyi* a relatively unique phenotypic plasmodial parasite. The described comparative features between *P. coatneyi*, *P. falciparum* and *P. vivax* are highlighted in Table 1.

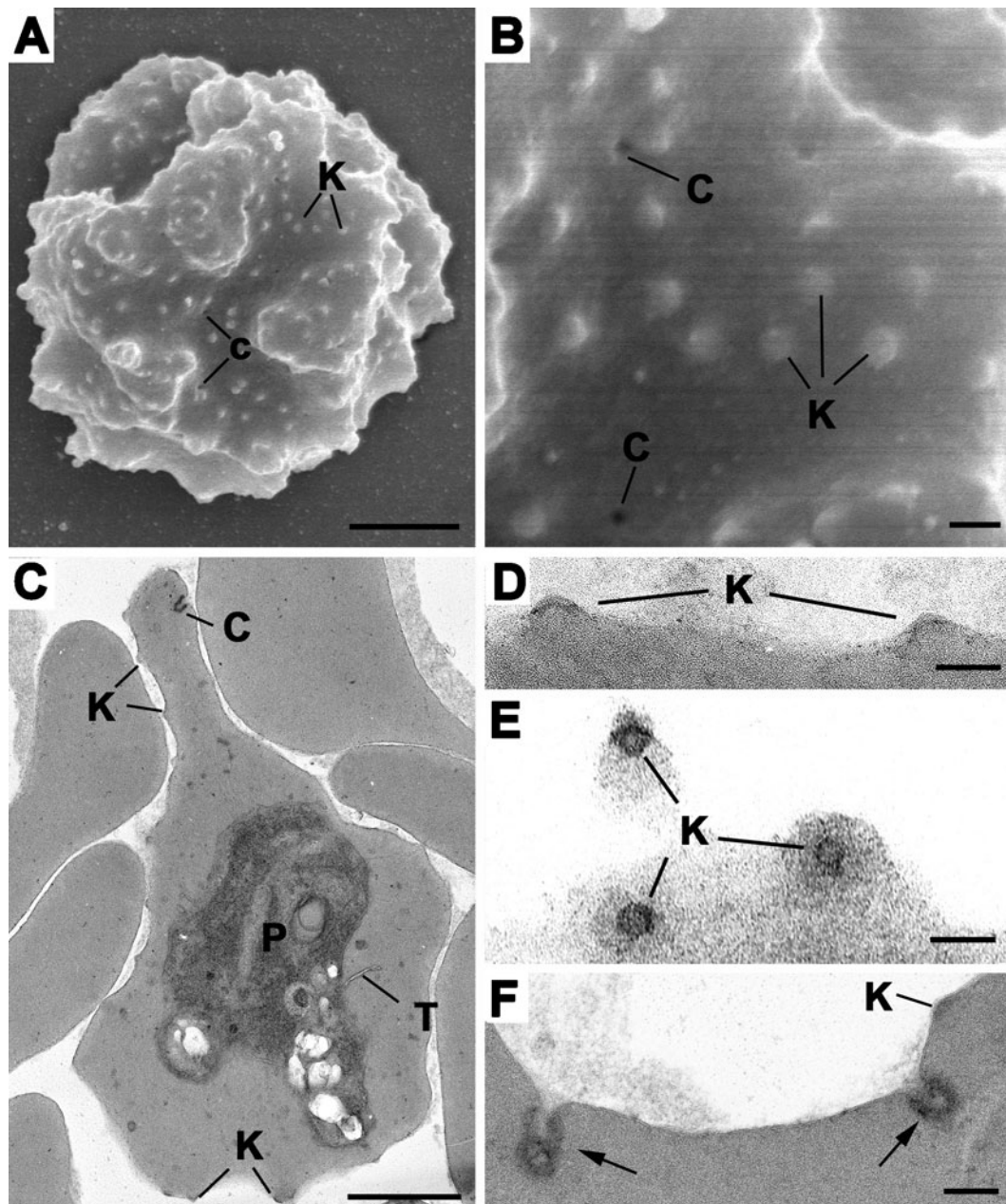


Fig. 4. Scanning electron (A, B) and transmission electron micrographs (C–F) of blood from *Plasmodium coatneyi* infected, spleen intact rhesus macaques. (A) Low power scanning electron micrograph of an iRBC showing the irregular (lumpy) surface appearance in which randomly distributed knobs (K) and caveolae (C) can be identified. Bar is 1 μ m. (B) Detail of the surface of the iRBC showing the circular slightly raised electron-lucent knobs (K) and the openings of the caveolae (C). Bar is 100 nm. (C) Low power image showing an iRBC containing a mid-stage trophozoite (P) in which tubular structures (T), caveolae (C) and knobs (K) can be identified. Bar is 1 μ m. (D) Longitudinal section through two knobs showing the underlying dense material (arrows). Bar is 100 nm. (E) Tangential section through the surface of an iRBC showing knobs (K) with the circular appearance of the underlying dense material. Bar is 100 nm. (F) Longitudinal section showing the caveolae formed by the invagination of the iRBC plasmalemma with underlying dense material (arrows). K – knob. Bar is 100 nm.

The knob-like structures of *P. falciparum* have been demonstrated to be involved in sequestration and specific adherence ligands have been identified at the knob (Cooke *et al.*, 2004; Horrocks *et al.*, 2005; Subramani *et al.*, 2015; Watermeyer *et al.*, 2016), and a similar association has been proposed in *P. coatneyi* infection (Kilejian *et al.*, 1977; Aikawa *et al.*, 1992; Kawai *et al.*, 2003). However, in the present study, the number and structure of the knobs appeared to be variable with some parasites having few knobs, which appeared to be independent of the stage of parasite development. The tissue samples examined in the present study were from splenectomized animals, which raises the question as to the effect of the absence of the spleen on the parasite. There has been renewed interest in the role of the spleen in both *P. vivax* and *P. falciparum* infections (Fernandez-Becerra

et al., 2020; Kho *et al.*, 2021) and a similar important role could be expected in *P. coatneyi* infections. In human *P. falciparum* infections, it is proposed that sequestration protects the parasite from clearance by avoiding passing through the spleen (Prommano *et al.*, 2005). It has also been noted that, in a splenectomized human infected with *P. falciparum*, the iRBC examined lacked knobs (Pongponratn *et al.*, 2000) although others reported their retention (Ho *et al.*, 1991). It has been shown that *P. falciparum* iRBCs lose their knobs in when cultured *in vitro* (Langreth *et al.*, 1979) and more recently it has been shown that culture conditions can have a marked effect on knob formation (Tilly *et al.*, 2015; Dörpinghaus *et al.*, 2020). This would suggest that the host factor affects the expression of knobs and, *in vivo*, this could involve the spleen. Previous experimental studies have used

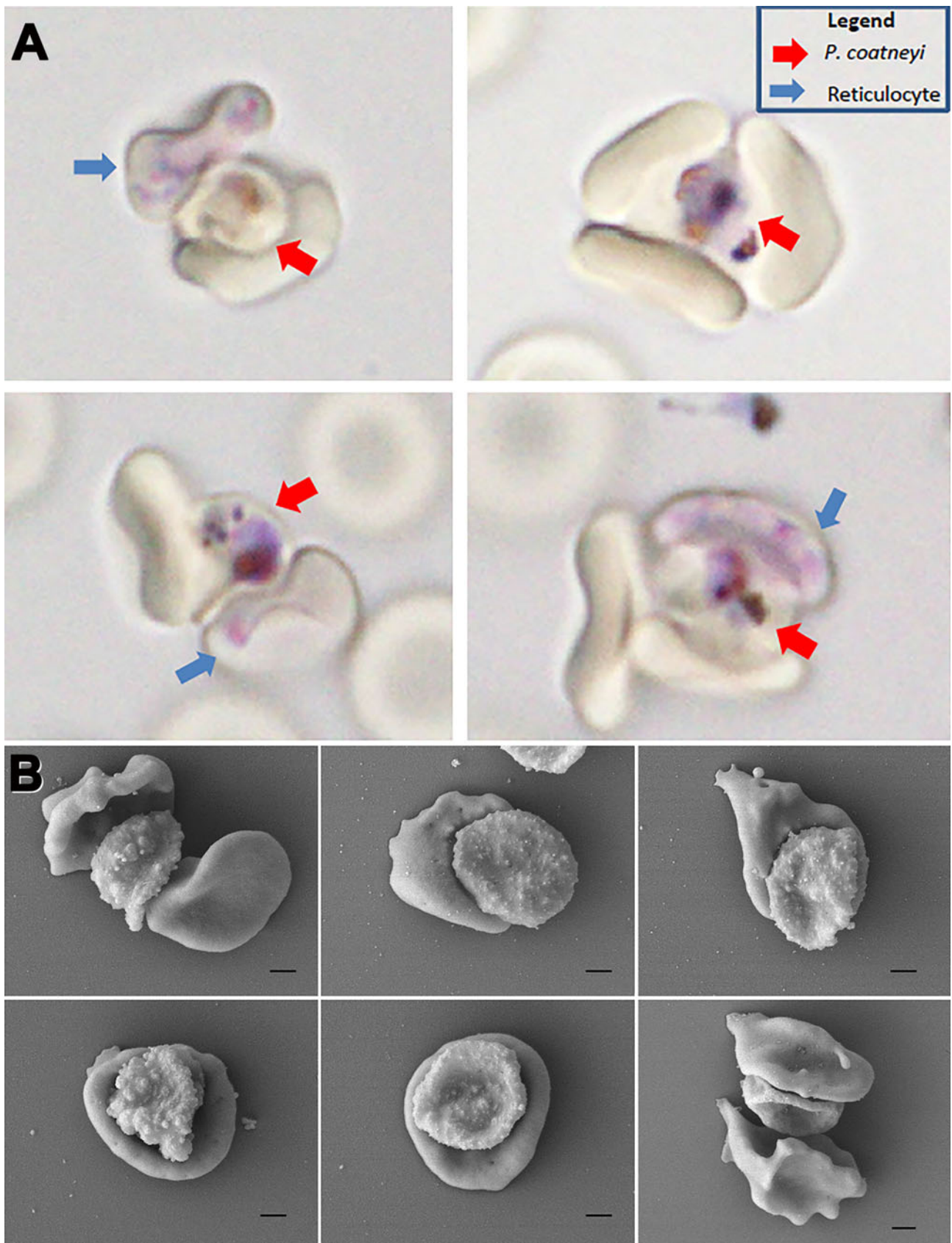


Fig. 5. *Plasmodium coatneyi* rosettes. (A) Giemsa-stained blood from *P. coatneyi* infected, spleen intact rhesus macaque rosettes. *P. coatneyi* rosettes with both normocytes and reticulocytes. Live-cell staining of rosettes under fluid conditions (Note *P. vivax* rosettes with normocytes only). (B) Scanning electron micrographs of blood from *P. coatneyi* infected, spleen-intact rhesus macaques (scale bar is 1 μm).

both spleen-intact and splenectomized animals, however, the ultrastructure of iRBCs was not directly compared in those studies (Eyles *et al.*, 1962; Desowitz *et al.*, 1967). In the present study,

there did appear to be some loss of the characteristic knob structures with variable loss of the underlying electron-dense material and/or the dome-shaped protuberance, which has not been

Table 1. Comparison of the ultrastructural features present in the cytoplasm of malaria plasmodial infected erythrocytes

Species	EM features			
	Knobs	Caveola	Maurer's clefts	Tubules/vesicular
<i>P. coatneyi</i>	+	+	–	+
<i>P. falciparum</i>	+	–	+	+
<i>P. vivax</i>	–	+ ^a	–	+

^aMore complex structures with associated vesicles.

reported previously. To investigate if such changes in the knobs could be related to the use of splenectomized animals, blood containing iRBCs of the same strain of *P. coatneyi* from spleen-intact animals was examined. It was found that iRBCs from spleen-intact animals possessed knobs with the characteristic substructure. This raises the possibility that the reduced selection pressure experienced in splenectomized animals could result in a progressive loss of intact knobs. The interaction of the iRBCs with endothelial cells with close apposition between the iRBC plasmalemma of the endothelial cell plasmalemma particularly at the site of knobs is similar to that seen with *P. falciparum* (MacPherson *et al.*, 1985; Pongponratn *et al.*, 2003). The cytoadherence of knob-negative parasites in the present study has not been reported for *P. falciparum* in spleen-intact patients (Pongponratn *et al.*, 2003). The structure of the knob involves multiple proteins both structural and adhesive ligands. *In vitro* studies have shown that certain strains of knob negative (loss of structural proteins) parasites can adhere to cultured endothelial cells and still express clumps of adhesive ligand at the surface in the absence of knobs (Horrocks *et al.*, 2005; Quadt *et al.*, 2012). Theoretically, it is possible that the variable changes observed in the knobs in the present study may represent a partial loss of knob proteins related to the lack of selection pressure associated with passage through the spleen, however additional investigation would be required to assess the further impact of parasite density and stage of parasite development on the development or loss of knobs in this model. The observation of rosettes between iRBCs and RBCs has been reported previously for *P. coatneyi* (Kilejian *et al.*, 1977; Udomsangpetch *et al.*, 1991; Aikawa *et al.*, 1992; Kawai *et al.*, 1995; Lombardini *et al.*, 2015) and is similar to that reported for certain isolates of *P. falciparum* (David *et al.*, 1988; Handunnetti *et al.*, 1989; Udomsangpetch *et al.*, 1989; Wahlgren *et al.*, 1989; Carlson *et al.*, 1990; Ho *et al.*, 1991; Carlson, 1993; Fernandez and Wahlgren, 2002). However, the formation of clumps of iRBCs (auto-agglutination) has not been reported before for *P. coatneyi* although this observation is similar to findings reported for certain isolates of *P. falciparum* (Hasler *et al.*, 1990; Roberts *et al.*, 2000; Fernandez and Wahlgren, 2002; Watermeyer *et al.*, 2016). Interestingly, *P. coatneyi* parasites seem to form rosettes with reticulocytes and normocytes when *P. falciparum* and *Plasmodium vivax* rosette primarily with normocytes (Lee *et al.*, 2014).

In conclusion, ultrastructural examination of *P. coatneyi* infection in the rhesus macaques demonstrated that the model replicates many of the host–parasite ultrastructural features associated with *P. falciparum* in humans and as such reinforces the potential suitability of this animal model for further studies of severe malaria. Those commonalities with *P. falciparum*, include the presence of knobs; tubular/vacuolar structures; close apposition to endothelial cells; interdigitating processes; similar parasite development; formation of rosettes and the formation

of auto-agglutinates. There are also important differences including the presence of caveolae; lack of Maurer's clefts; no evidence of tissue-specific sequestration; and examples of incomplete knob formation.

It is important to note the possibility that the use of splenectomized animals in this and other *P. coatneyi* studies could compromise the observed similarities with falciparum malaria in infected humans and should be considered in the development of future studies and further refinement of this animal model.

Acknowledgements. We are extremely grateful to the generations of researchers and scientists who have laboured towards a greater understanding of *P. coatneyi* malaria, to the staff of the Department of Veterinary Medicine of AFRIMS, and to constructive discussions and advice of Professor Nick White, Mahidol Oxford Tropical Medicine Research Unit and the University of Oxford. Additionally, the authors acknowledge the Electron Microscopy Unit (EMU), the National University of Singapore, and particularly thank Miss Tan Suat Hoon.

Author contributions.

EL, AB and GT conceived and designed the study; AR, NP and TK were critical in the technical performance and data gathering of the study; EL, GT, BR, BM and DF performed data analysis and EL, AB, GT, BM, BR and DF wrote the article.

Financial support. Grant support from the Wellcome Trust of Great Britain (grant 089275/Z/09/Z). Benoit Malleret was funded by NUHS Start-up grant (NUHSRO/2018/006/SU/01) and core funds to SiGN from A*STAR and Mister Lu Thong Beng.

Conflict of interest. E. D. Lombardini is a Colonel in the United States Army. The opinions or assertions herein are those of the authors and do not necessarily reflect the view of the Department of the Army or the Department of Defense. Otherwise, the authors declare there are no conflicts of interest.

Ethical standards. The research was conducted in strict compliance with the United States Animal Welfare Act and other federal statutes and regulations relating to animals and experiments involving animals and adhered to principles stated in the Guide for the Care and Use of Laboratory Animals, NRC Publication, 2011 edition. All animal use was approved by the AFRIMS Institutional Animal Care and Use Committee Protocol Number 12-08.

References

- Aikawa M (1988a) Human cerebral malaria. *American Journal of Tropical Medicine and Hygiene* **39**, 1–10.
- Aikawa M (1988b) Morphological changes in erythrocytes induced by malarial parasites. *Biology of the Cell* **64**, 173–181.
- Aikawa M, Miller LH and Rabbege J (1975) Caveola-vesicle complexes in the plasmalemma of erythrocytes infected by *Plasmodium vivax* and *P. cynomolgi*. Unique structures related to Schüffner's dots. *American Journal of Pathology* **79**, 285–300.
- Aikawa M, Rabbege JR, Udeinya I and Miller LH (1983) Electron microscopy of knobs in *Plasmodium falciparum*-infected erythrocytes. *Journal of Parasitology* **69**, 435–437.
- Aikawa M, Udeinya IJ, Rabbege J, Dayan M, Leech JH, Howard RJ and Miller LH (1985) Structural alteration of the membrane of erythrocytes infected with *Plasmodium falciparum*. *Journal of Protozoology* **32**, 424–429.
- Aikawa M, Brown AE, Smith CD, Tegoshi T, Howard RJ, Hasler TH, Ito Y, Collins WE and Webster HK (1992) *Plasmodium coatneyi*-infected rhesus monkeys: a primate model for human cerebral malaria. *Instituto Oswaldo Cruz* **87**(Suppl. 3), 443–447.
- Aikawa M, Hanssen E, Meyer EV, Jiang J, Korir CC, Singh B, Lapp S, Barnwell JW, Tilley L and Galinski MR (2012) A 95 kDa protein of *Plasmodium vivax* and *P. cynomolgi* visualized by three-dimensional tomography in the caveola-vesicle complexes (Schuffner's dots) of infected erythrocytes is a member of the PHIST family. *Molecular Microbiology* **84**, 816–831.
- Atkinson CT and Aikawa M (1990) Ultrastructure of malaria-infected erythrocytes. *Blood Cells* **16**, 351–368.
- Bannister LH, Hopkins JM, Fowler RE, Krishna S and Mitchell GH (2000) A brief illustrated guide to the ultrastructure of *Plasmodium falciparum* asexual blood stages. *Parasitology Today* **16**, 427–433.

- Barnwell JW, Ingravallo P, Galinski MR, Matsumoto Y and Aikawa M (1990) *Plasmodium vivax*: malarial proteins associated with the membrane-bound caveola-vesicle complexes and cytoplasmic cleft structures of infected erythrocytes. *Experimental Parasitology* **70**, 85–99.
- Carlson J (1993) Erythrocyte rosetting in *Plasmodium falciparum* malaria with special reference to the pathogenesis of cerebral malaria. *Scandinavian Journal of Infectious Diseases Supplement* **86**, 1–79.
- Carlson J, Helmsby H, Hill AV, Brewster D, Greenwood BM and Wahlgren M (1990) Human cerebral malaria: association with erythrocyte rosetting and lack of anti-rosetting antibodies. *Lancet (London, England)* **336**, 1457–1460.
- Cooke BM, Mohandas N and Coppel RL (2004) Malaria and the red blood cell membrane. *Hematology (Amsterdam, Netherlands)* **41**, 173–188.
- David PH, Handunnetti SM, Leech JH, Gamage P and Mendis KN (1988) Rosetting: a new cytoadherence property of malaria-infected erythrocytes. *American Journal of Tropical Medicine and Hygiene* **38**, 289–297.
- Desowitz RS, Miller LH, Buchanan RD, Yuthasastrkosol V and Permpnich B (1967) Comparative studies on the pathology and host physiology of malarias: I. *Plasmodium coatneyi*. *Annals of Tropical Medicine and Parasitology* **61**, 365–374.
- Desowitz RS, Miller LH, Buchanan RD and Permpnich B (1969) The sites of deep vascular schizogony in *Plasmodium coatneyi* malaria. *Transactions of The Royal Society of Tropical Medicine and Hygiene* **63**, 198–202.
- Dörpinghaus M, Fürstenwerth F, Roth LK, Bouws P, Rakotonirinalalao M, Jordan V, Sauer M, Rehn T, Pansegrau E, Höhn K, Mesén-Ramírez P, Bachmann A, Lorenzen S, Roeder T, Metwally NG and Bruchhaus I (2020) Stringent selection of knobby *Plasmodium falciparum*-infected erythrocytes during cytoadhesion at febrile temperature. *Microorganisms* **8**, 174.
- Escalante AA, Barrio E and Ayala FJ (1995) Evolutionary origin of human and primate malarias: evidence from the circumsporozoite protein gene. *Molecular Biology and Evolution* **12**, 616–626.
- Eyles DE, Fong YL, Warren M, Guinn E, Sandosham AA and Wharton R (1962) *Plasmodium coatneyi*, a new species of primate malaria from Malaya. *American Journal of Tropical Medicine and Hygiene* **11**, 597–604.
- Eyles DE, Dunn FL, Warren M and Guinn E (1963) *Plasmodium coatneyi* from the Philippines. *Journal of Parasitology* **49**, 1038.
- Eyles DE, Fong YL, Warren M, Guinn EG, Sandosham AA and Wharton RH (1971) *Plasmodium coatneyi*. In Coatney GR, Collins WE, Warren M and Contacos PG (eds), *The Primate Malarias*. Washington, DC, USA: Government Printing Office, pp. 289–299.
- Fernandez-Becerra C, Bernabeu M, Castellanos A, Bruna R, Correa BR, Obadia T, Ramirez M, Rui E, Hentzschel F, López-Montañés M, Ayllon-Hermida A, Martin-Jaular L, Elizalde-Torrent A, Siba P, Vêncio RZ, Arevalo-Herrera M, Herrera S, Alonso PL, Mueller I and del Portillo HA (2020) *Plasmodium vivax* spleen-dependent genes encode antigens associated with cytoadhesion and clinical protection. *Proceedings of the National Academy of Sciences USA* **117**, 13056–13065.
- Fernandez V and Wahlgren M (2002) Rosetting and autoagglutination in *Plasmodium falciparum*. *Chemical Immunology* **80**, 163–187.
- Handunnetti SM, David PH, Perera KL and Mendis KN (1989) Uninfected erythrocytes form “rosettes” around *Plasmodium falciparum* infected erythrocytes. *American Journal of Tropical Medicine and Hygiene* **40**, 115–118.
- Hasler T, Handunnetti SM, Aguiar JC, van Schravendijk MR, Greenwood BM, Lalliger G, Cegielski P and Howard RJ (1990) In vitro rosetting, cytoadherence, and microagglutination properties of *Plasmodium falciparum*-infected erythrocytes from Gambian and Tanzanian patients. *Blood* **76**, 1845–1852.
- Hayakawa T, Culleton R, Otani H, Horii T and Tanabe K (2008) Big bang in the evolution of extant malaria parasites. *Molecular Biology and Evolution* **25**, 2233–2239.
- Ho M, Davis TM, Silamut K, Bunnag D and White NJ (1991) Rosette formation of *Plasmodium falciparum*-infected erythrocytes from patients with acute malaria. *Infection and Immunity* **59**, 2135–2139.
- Horrocks P, Pinches RA, Chakravorty SJ, Papakrivovs J, Christodoulou Z, Kyes SE, Urban BC, Ferguson DJP and Newbold CI (2005) PfEMP1 expression is reduced on the surface of knobless *Plasmodium falciparum* infected erythrocytes. *Journal of Cell Science* **118**(Pt 11), 2507–2518.
- Kawai S, Aikawa M, Kano S and Suzuki M (1993) A primate model for severe human malaria with cerebral involvement: *Plasmodium coatneyi*-infected *Macaca fuscata*. *American Journal of Tropical Medicine and Hygiene* **48**, 630–636.
- Kawai S, Kano S and Suzuki M (1995) Rosette formation by *Plasmodium coatneyi*-infected erythrocytes of the Japanese macaque (*Macaca fuscata*). *American Journal of Tropical Medicine and Hygiene* **53**, 295–299.
- Kawai S, Aikawa M, Suzuki M and Matsuda H (1998) A nonhuman primate model for severe human malaria: *Plasmodium coatneyi*-infected Japanese macaque (*Macaca fuscata*). *The Tokai Journal of Experimental and Clinical Medicine* **23**, 101–102.
- Kawai S, Matsumoto J, Aikawa M and Matsuda H (2003) Increased plasma levels of soluble intercellular adhesion molecule-1 (sICAM-1) and soluble vascular cell molecule-1 (sVCAM-1) associated with disease severity in a primate model for severe human malaria: *Plasmodium coatneyi*-infected Japanese macaques (*Macaca fuscata*). *Journal of Veterinary Medical Science* **65**, 629–631.
- Kho S, Qotrunnada L, Leonardo L, Andries B, Wardani PAI, Fricot A, Henry B, Hardy D, Margyaningsih NI, Apriyanti D, Puspitasari AM, Prayoga P, Trianty L, Kenangalem E, Chretien F, Brousse V, Safeukui I, del Portillo HA, Fernandez-Becerra C, Meibalan E, Marti M, Price RN, Woodberry T, Ndour PA, Russell BM, Yeo TW, Minigo G, Noviyanti R, Poespoprodjo JR, Siregar NC, Buffet PA and Anstey NM (2021) Evaluation of splenic accumulation and colocalization of immature reticulocytes and *Plasmodium vivax* in asymptomatic malaria: a prospective human splenectomy study. *PLoS Medicine* **18**, e1003632.
- Kilejian A, Abati A and Trager W (1977) *Plasmodium falciparum* and *Plasmodium coatneyi*: immunogenicity of “knob-like protrusions” on infected erythrocyte membranes. *Experimental Parasitology* **42**, 157–164.
- Langreth SG, Reese RT, Motyl MR and Trager W (1979) *Plasmodium falciparum*: loss of knobs on the infected erythrocyte surface after long-term cultivation. *Experimental Parasitology* **48**, 213–219.
- Leclerc MC, Hugot JP, Durand P and Renaud F (2004) Evolutionary relationships between 15 *Plasmodium* species from new and old-world primates (including humans): an 18S rDNA cladistic analysis. *Parasitology* **129**(Pt 6), 677–684.
- Lee W-C, Russell B, Lau Y-L, Fong M-Y, Chu C, Sriprawatt K, Suwanarusk R, Nosten F and Renia L (2013) Giemsa-stained wet mount based method for reticulocyte quantification: a viable alternative in resource-limited or malaria-endemic settings. *PLoS ONE* **8**, e60303.
- Lee WC, Malleret B, Lau Y-L, Mauduit M, Fong M-Y, Cho JS, Suwanarusk R, Zhang R, Albrecht L, Costa FTM, Preiser P, McGready R, Renia L, Nosten F and Russell B (2014) Glycophorin C (CD236R) mediates vivax malaria parasite rosetting to normocytes [published correction appears in *Blood*. 2015; 126, 2765]. *Blood* **123**, e100–e109.
- Liu B, Blanch AJ, Namvar A, Carmo O, Tiash S, Andrew D, Hanssen E, Rajagopal V, Dixon MWA and Tilley L (2019) Multimodal analysis of *Plasmodium knowlesi*-infected erythrocytes reveals large invaginations, swelling of the host cell, and rheological defects. *Cell Microbiology* **21**, e13005.
- Lombardini ED, Gettayacamin M, Turner GDH and Brown AE (2015) A review of *Plasmodium coatneyi*-macaque models of severe and cerebral malaria. *Veterinary Pathology* **52**, 998–1011.
- Lombardini ED, Turner GDH, Brown AE, Inamnuay L, Kaewamatawong T, Sunyakumthorn P and Ferguson DJP (2021) Systemic ultrastructural tissue pathology of *Plasmodium coatneyi* infection in rhesus macaques. *Veterinary Pathology* (accepted for publication).
- MacPherson GG, Warrell MJ, White NJ, Looareesuwan S and Warrell DA (1985) Human cerebral malaria. A quantitative ultrastructural analysis of parasitized erythrocyte sequestration. *American Journal of Pathology* **119**, 385–401.
- Maeno Y, Brown AE, Smith CD, Tegoshi T, Toyoshima T, Ockenhouse C, Corcoran K, Ngampochjana M, Kyle D and Webster H (1993) A non-human primate model for cerebral malaria: effects of artesunate (qinghaosu derivative) on rhesus monkeys experimentally infected with *Plasmodium coatneyi*. *American Journal of Tropical Medicine and Hygiene* **49**, 726–734.
- Malleret B, Xu F, Mohandas N, Suwanarusk R, Chu C, Leite JA, Low K, Turner C, Sriprawatt K, Zhang R, Bertrand O, Colin Y, Costa FTM, Ong CN, Ng ML, Lim CT, Nosten F, Renia L and Russell B (2013) Significant biochemical, biophysical and metabolic diversity in circulating human cord blood reticulocytes. *PLoS One* **8**, e76062.
- Moreno A, Cabrera-Mora M, Garcia A, Orkin J, Strobert E, Barnwell JW and Galinski MR (2013) *Plasmodium coatneyi* in rhesus macaques replicates the multisystemic dysfunction of severe malaria in humans. *Infection and Immunity* **81**, 1889–1904.

- Mundwiler-Pachlatko E and Beck HP** (2013) Maurer's clefts, the enigma of *Plasmodium falciparum*. *Proceedings of the National Academy of Sciences USA* **110**, 19987–19994.
- Nguansangiam S, Day NP, Hien TT, Mai NTH, Chaisri U, Riganti M, Dondorp AM, Lee SJ, Phu NH, Turner GDH, White NJ, Ferguson DJP and Pongponratn E** (2007) A quantitative ultrastructural study of renal pathology in fatal *Plasmodium falciparum* malaria. *Tropical Medicine and International Health* **12**, 1037–1050.
- Pongponratn E, Riganti M, Punpoowong B and Aikawa M** (1991) Microvascular sequestration of parasitized erythrocytes in human falciparum malaria: a pathological study. *American Journal of Tropical Medicine and Hygiene* **44**, 168–175.
- Pongponratn E, Viriyavejakul P, Wilairatana P, Ferguson DJP, Chaisri U, Turner GDH and Looareesuwan S** (2000) Absence of knobs on parasitized red blood cells in a splenectomized patient in fatal falciparum malaria. *Southeast Asian Journal of Tropical Medicine and Public Health* **31**, 829–835.
- Pongponratn E, Turner GDH, Day NP, Phu NH, Simpson JA, Stepniewska K, Mai NTH, Viriyavejakul P, Looareesuwan S, Hien TT, Ferguson DJP and White NJ** (2003) An ultrastructural study of the brain in fatal *Plasmodium falciparum* malaria. *American Journal of Tropical Medicine and Hygiene* **69**, 345–359.
- Prommano O, Chaisri U, Turner GDH, Wilairatana P, Ferguson DJP, Viriyavejakul P, White NJ and Pongponratn E** (2005) A quantitative ultrastructural study of the liver and the spleen in fatal falciparum malaria. *Southeast Asian Journal of Tropical Medicine and Public Health* **36**, 1359–1370.
- Quadt KA, Barfod L, Andersen D, Bruun J, Gyan B, Hassenkam T, Ofori MF and Hviid L** (2012) The density of knobs on *Plasmodium falciparum*-infected erythrocytes depends on developmental age and varies among isolates. *PLoS One* **7**, e45658.
- Roberts DJ, Pain A, Kai O, Kortok M and Marsh K** (2000) Autoagglutination of malaria-infected red blood cells and malaria severity. *Lancet (London, England)* **355**, 1427–1428.
- Sein KK, Brown AE, Maeno Y, Smith CD, Corcoran KD, Hansukjariya P, Webster HK and Aikawa M** (1993) Sequestration pattern of parasitized erythrocytes in cerebrum, mid-brain and cerebellum of *Plasmodium coatneyi*-infected rhesus monkeys (*Macaca mulatta*). *American Journal of Tropical Medicine and Hygiene* **49**, 513–519.
- Smith CD, Brown AE, Nakazawa S, Fujioka H and Aikawa M** (1996) Multi-organ erythrocyte sequestration and ligand expression in rhesus monkeys infected with *Plasmodium coatneyi* malaria. *American Journal of Tropical Medicine and Hygiene* **55**, 379–383.
- Subramani R, Quadt K, Jeppesen AE, Hempel C, Petersen JEV, Hassenkam T, Hviid L and Barfod L** (2015) *Plasmodium falciparum*-infected erythrocyte knob density is linked to the PfEMP1 variant expressed. *MBio* **6**, e01456-15.
- Tegoshi T, Udomsangpetch R, Brown AE, Nakazawa S, Webster HK and Aikawa M** (1993) Ultrastructure of rosette formation by *Plasmodium coatneyi*-infected erythrocytes of rhesus. *Parasitology Research* **79**, 611–613.
- Tilly AK, Thiede J, Metwally N, Lubiana P, Bachmann A, Roeder T, Rockcliffe N, Lorenzen S, Tannich E, Gutsmann T and Bruchhaus I** (2015) Type of in vitro cultivation influences cytoadhesion, knob structure, protein localization and transcriptome profile of *Plasmodium falciparum*. *Scientific Reports* **5**, 16766.
- Udagama PV, Atkinson CT, Peiris JS, David PH, Mendis KN and Aikawa M** (1988) Immunoelectron microscopy of Schuffner's dots in *Plasmodium vivax*-infected human erythrocytes. *American Journal of Pathology* **131**, 48–52.
- Udomsangpetch R, Wählin B, Carlson J, Berzins K, Torri M, Aikawa M, Perlmann P and Wahlgren M** (1989) *Plasmodium falciparum*-infected erythrocytes form spontaneous erythrocyte rosettes. *Journal of Experimental Medicine* **169**, 1835–1840.
- Udomsangpetch R, Brown AE, Smith CD and Webster HK** (1991) Rosette formation by *Plasmodium coatneyi*-infected red blood cells. *American Journal of Tropical Medicine and Hygiene* **44**, 399–401.
- Wahlgren M, Carlson J, Udomsangpetch R and Perlmann P** (1989) Why do *Plasmodium falciparum*-infected erythrocytes form spontaneous erythrocyte rosettes? *Parasitology Today* **5**, 183–185.
- Watermeyer JM, Hale VL, Hackett F, Clare DK, Cutts EE, Vakonakis I, Fleck RA, Blackman MJ and Saibil HR** (2016) A spiral scaffold underlies cytoadherent knobs in *Plasmodium falciparum*-infected erythrocytes. *Blood* **127**, 343–351.